circ_0000018 downregulation peripherally ameliorates neuroprotection against acute ischemic stroke through the miR-871/BCL2L11 axis

MIN JIANG, XIAO-BIN WANG and SHAN JIANG

Laboratory Animal Centre, Southeastern University, Nanjing, Jiangsu 210003, P.R. China

Received March 20, 2023; Accepted September 6, 2023

DOI: 10.3892/mmr.2023.13107

Abstract. Acute ischemic stroke (AIS) is a common acute cerebrovascular disease. Circular RNAs (circRNAs) have been demonstrated to have critical functions in a wide range of physiological processes and disorders in humans. However, their precise function in ischemic stroke (IS) remains largely unknown. The present study explored the function and potential mechanisms of circ_0000018 in AIS *in vivo* and *in vitro*. The cerebral ischemia/reperfusion injury model was established *in vivo* and *in vitro* using the oxygen-glucose deprivation (OGD/R) and transient middle cerebral artery occlusion (tMCAO) methods. Subsequently, the impact of circ_0000018 on cerebral ischemia/reperfusion injury was assessed using various techniques, including TTC staining, quantitative PCR, western blotting, cell counting kit-8 assay, Annexin V-FITC Apoptosis Detection Kit, luciferase reporter gene assays, and others. The levels of circ_0000018 were markedly increased in the OGD/R-treated neuronal cells and in a mouse model of tMCAO. The blocking of microRNA (miR)-871 by circ_0000018 promoted Bcl-2-like protein 11 (BCL2L11) expression to increase neuronal cell damage. Furthermore, circ_0000018 knockdown significantly improved neuronal cell viability and attenuated OGD/R-treated neuronal cell death. Meanwhile, circ_0000018 knockdown improved brain infarct volume and neuronal apoptosis in tMCAO mice. The present study found that circ_0000018 knockdown relieved cerebral ischemia-reperfusion injury progression *in vitro* and *in vivo*. Mechanistically, circ_0000018 regulated the levels of BCL2L11 by sponging miR-871.

Correspondence to: Dr Xiao-Bin Wang, Laboratory Animal Centre, Southeastern University, 87 Dingjiaqiao, Nanjing, Jiangsu 210003, P.R. China
E-mail: dwzx2887@163.com

Key words: acute ischemic stroke, circ_0000018, microRNA-871, Bcl-2-like protein 11

Introduction

Ischemic stroke (IS) is the leading cause of long-term disability and a major cause of morbidity and mortality worldwide (1,2). Acute ischemic stroke (AIS) accounts for ~81.9% of the total number of strokes (3). With high morbidity, disability, recurrence, and mortality rates. AIS may pose a serious threat to human life and health due to impaired blood flow to the brain, ischemia, and hypoxia (4,5). This mechanism may be involved in atherosclerosis, dyslipidemia, and hemodynamic changes in blood composition. Previous studies have found that the ischemia and hypoxia-induced injury cascade is the key cause of tissue damage and long-term neurological dysfunction following cerebral ischemia. Neuronal injury caused by AIS directly leads to brain parenchymal injury, and neurons are important target cells for stroke treatment. Therefore, studying nerve injury and the neuroprotective mechanism of stroke is of particular importance.

Circular RNAs (circRNAs) are a relatively newfound class of endogenous non-coding RNAs, and are covalently bonded closed loops of RNA through a special splicing mechanism. CircRNAs are widely expressed in eukaryotes, and this expression is highly conserved, and tissue and spatiotemporal-specific. Due to the special closed ring structure, circRNAs are less susceptible to degradation by exonucleases and are more stable than linear RNAs (6,7). At present, the evaluation of the effect of circRNAs in ischemic brain injury is still in the initial stages. It has been reported that a few distinctly expressed circRNAs were identified in an AIS model (8-10). However, the mechanisms remain incompletely understood.

Numerous studies have shown that miRNAs can be used for a variety of diseases as therapeutic targets and biomarkers (11-13). In fact, miRNAs can also be detected in several central nervous system diseases, including Parkinson's disease, Down's syndrome, schizophrenia, and stroke (14-18). According to previous reports (19), miRNAs are endogenously expressed RNA molecules that have an important effect in regulating the pathophysiological process of cerebral infarction, and the expression levels of miRNAs in the blood can reflect brain damage and recovery in patients with cerebral infarcts.

In the present study, the functions of circ_0000018 in neuronal cell apoptosis in AIS progression were explored *in vivo* and *in vitro*. It was found that circ_0000018 knockdown alleviated neuronal cell apoptosis by targeting the

miR-871/Bcl-2-like protein 11 (BCL2L11) axis, indicating that circ_0000018 may serve as a potential strategy for inducing neuroprotective AIS.

Materials and methods

Analysis of microarrays. A Gene Expression Omnibus (GEO) (https://www.ncbi.nlm.nih.gov/geo/) dataset (GSE115697) that assessed circRNA expression patterns in NSCLC and was analyzed by using GEO2R (https://www.ncbi. nlm.nih.gov/geo/geo2r/) was obtained and used in the present study (20). Raw data were normalized by Quantile algorithm, limma package the R program (21). R software (version 4.0.3) was used for the data download and processing (22). The 'GEOquery' package was used to download the dataset expression matrix and platform file. The 'limma' package was used for differential analysis of microarray data. After confirming that the quality of the samples, the subsequent difference analysis was performed. Significant differentially expressed transcripts were screened using $P<0.05$ and fold-change ≥ 0.5 or ≤ -1 The 'ggplot2' package was used to visualize the heatmap and volcano plot.

Cell culture and establishment of the oxygen-glucose deprivation/reperfusion (OGD/R) model. The mouse neuroblast (Neuro-2a cells; https://www.atcc.org/products/ccl-131) were obtained from the American Type Culture Collection. Mouse neuronal cells were cultured in DMEM (Invitrogen; Thermo Fisher Scientific, Inc.) supplemented with 10% FBS (Invitrogen; Thermo Fisher Scientific, Inc.) and antibiotics (100 U/ml penicillin, 100 μg/ml streptomycin, PAN Biotech), and maintained in a humidified incubator at 37˚C and supplied with 5% CO_2 air.

For the establishment of the OGD/R cell model, the original culture medium was discarded, the neuronal cells were washed with PBS, placed in sugar-free DMEM medium without FBS, and incubated as above for 2 h. Next, the media was removed, and supplemented DMEM was added, and the cells were transferred to an incubator supplied with air consisting of 95% N_2, 5% CO_2, and 1% O_2 for 6 h (23). Subsequently, the media was replaced with supplemented DMEM and transferred back to the previous conditions for 12 h. In addition, cells cultured in normal DMEM at 37˚C with 5% CO_2 in a humidified incubator were used as the control.

Cell transfection. To induce circ_0000018 knockdown, OGD/R-treated cells and control cells were transfected with 50 nM circ_0000018 small interference RNA (si-circ_0000018; Guangzhou RiboBio Co., Ltd.) or non-targeting siRNA (si-NC, Guangzhou RiboBio Co., Ltd.). Similarly, 50 nM miR-871 mimic (agomiR-871), miR-871 inhibitor (antagomiR-871) and their blank controls (miR-NC and anti-miR-NC; all from Guangzhou RiboBio Co., Ltd.) were respectively transfected into neuronal cells. The overexpression vector (pcDNA-BCL2L11) was obtained by inserting the BCL2-like 11 overexpressed CDS sequence (oe-BCL2L11) into a pcDNA vector (Invitrogen; Thermo Fisher Scientific, Inc.), and the empty vector was used as the negative control. A total of 200 ng vector was transfected into neuronal cells using Lipofectamine® 3000 (Invitrogen; Thermo Fisher Scientific, Inc.).

Establishment of the transient middle cerebral artery occlusion (tMCAO) model. Male C57BL/6J mice (7-8 weeks, 18-25 g) were obtained from Beijing Vital River Laboratory Animal Technology Co., Ltd. The animals were randomly separated into groups and kept in a temperature-controlled room at 25±2˚C with a 40-50% relative humidity and a 12 h light/dark cycle. All experimental procedures were approved by the Southeast University Animal Care and Use Committee (approval no. 20220110026).

The mice were randomly allocated into a sham group, tMCAO group, tMCAO+sh-NC group, or tMCAO+sh-circ_0000018 group (n=18 per group). After 7 days of acclimatization, a model of cerebral AIS was created in mice by tMCAO with modifications based on earlier reports (24,25). Briefly, 1% sodium pentobarbital (50 mg/kg) was injected intraperitoneally to anesthetize the mice. Following a midline skin incision, the right common carotid artery, external carotid artery, and internal carotid artery (ICA) were explanted, and the L1800 silicone wire (Jialing Biotechnology Co., Ltd.) was then inserted 10 mm into the ICA to obscure the origin of the MCA. Brain reperfusion was performed by withdrawing silicone filaments after 90 min. In the sham group, the mice underwent the same tMCAO procedure but without ICA occlusion. The sh-NC and sh-circ_0000018 (Shanghai GenePharma Co., Ltd.) were injected into the lateral ventricle 1 day prior to tMCAO. Throughout the procedure, the temperature of the rectum of the mice was kept at 37.0±0.5˚C using a heat lamp (Jiaxing Nomoy Pet Products Co., Ltd.). Following the neurobehavioral scoring of all mice, the mice were euthanized by inhalation of carbon dioxide (35% volume displacement rate/min) inhalation following isoflurane anesthesia (induction percentage, 3%; maintenance percentage, 1%), and brain tissue was obtained for subsequent experiments.

Evaluation of neurological impairment. The neurological deficits of mice were evaluated using the Longa biologic score 24 h after 1 h of brain ischemia and reperfusion (26). The scoring system used was: 0, both forelimbs are strong and symmetrically extended to the ground, both shoulders have the same resistance, and walking is normal; 1, internal rotation on the contralateral side of the surgery, forelimb tucked in, both shoulders resist in unison, and walking is normal; 2, internal rotation on the contralateral side of the surgery, forelimb inversion, decreased resistance on the contralateral side of the surgery when pushing both shoulders, and walking is normal; 3, when the surgical contralateral side is internally rotated, the forelimb is tucked in, and both shoulders are pushed; when pushing both shoulders, the resistance of the contralateral side of the surgery decreases, mice can walk around; and 4, no spontaneous movement on the opposite side of the surgery. The observers were blinded to the treatment.

TTC staining. After assessment of neurological damage, mice were euthanized by CO_2 inhalation following halothane anesthesia, and brains were rapidly collected, cut into 2-mm sections, and incubated with 2% TTC solution (MilliporeSigma) at 37˚C for 10 min. Subsequently, 4% paraformaldehyde was used to fix the brain tissue for 1-2 days at room temperature, and then an image was taken. The infarct volume was calculated

using ImageJ 1.8.0.345 (National Institutes of Health). Normal brain tissue appeared red when TTC reacted with dehydrogenase, while in the ischemic brain tissue, it appeared white due to reduced dehydrogenase activity. The infarct volume ratio as a percentage was calculated as follows: Infarct volume (%)=[(Sum of infarct area x2 mm^3)/(sum of total brain area x2 mm^3) x100.

Reverse transcription-quantitative PCR (RT-qPCR). Total RNA was isolated from cultured cells, serum, and brain tissue using TRIzol® reagent according to the manufacturer's protocol (Invitrogen; Thermo Fisher Scientific, Inc.). The PrimeScript RT kit was used to reverse transcribe total RNA to cDNA according to the manufacturer's protocol (Takara Bio, Inc.). The levels of circ_0000018, miR-871, and BCL2L11 were measured using qPCR with a SYBR green kit (Takara Bio, Inc.) in a Bio-Rad CFX96 system (Bio-Rad, Laboratories, Inc.). The procedure was as follows: 95˚C for 3 min; followed by 39 cycles of 95˚C for 15 sec, 60˚C for 60 sec and 72˚C-30 sec for mRNA, or 95˚C for 15 sec and 60˚C for 60 sec for miRNA; 95˚C for 10 sec, followed by a melt curve analysis (60-95˚C, 0.5˚C increments for 20 sec) to confirm specificity of the PCR primers. The expression levels were normalized to the expressions of β-actin or U6. The $2^{-\Delta\Delta Cq}$ method was used to determine gene expression in the neuronal cells and brain tissues (27).

The sequences of the primers used were: circ_0000018 forward, 5'-CAAGATCACCTCCGATTGGT-3' and reverse, 5'-TGTCTTCTGCTCCAGGATCTTT-3'; miR-871 forward, 5'-TGCGGTCTGACCGTGGTAAGACC-3' and reverse, 5'-CCAGTGCAGGGTCCGAGGT-3'; BCL2L11 forward, 5'-CCCGGAGATACGGATTGCAC-3' and reverse, 5'-GCC TCGCGGTAATCATTTGC-3; and U6 forward, 5'-CTCGCT TCGGCAGCAC-3' and reverse, 5'-ACGCTTCACGAATTT GC-3'; cicr_0001646 forward, 5'-GGCAGATGGAAGCTT CTTGA-3' and reverse, 5'-AGCAAGTTGACCCATTTT CC-3'.

Western blot analysis. Total protein was extracted from cells using RIPA lysis buffer (Cell Signaling Technology, Inc.) and quantified using a BCA Protein Quantification Kit (Abbkine Scientific Co., Ltd.). Equivalent quantities of protein (30 μg) was loaded per lane on a 10% SDS-gel, resolved using SDS-PAGE, and transferred onto PVDF membranes (MilliporeSigma), followed by blocking with 5% milk in TBST at room temperature for 2 h, and subsequent incubation with one of the primary antibodies at 4˚C overnight. The corresponding secondary antibodies were used to incubate the membranes for 1 h at room temperature, followed by visualization using a chemiluminescence detection kit (Beyotime Institute of Biotechnology). The primary antibodies used in the present study were: Toll-like receptor 4 (TLR4; ab22048; 1:300), β-tubulin III (ab18207; 1:3,000), Bax (ab32503; 1;300), Bcl-2 (ab182858; 1:3,000), Caspase-3 (ab32351; 1:1,000), H2A.X Variant Histone (H2AX) (ab124781; 1:1,000), γH2AX (ab81299; 1:5,000) and β-actin (ab8226; 1:1,000) (all Abcam). The secondary antibody used in the present study were as follows: HRP-Conjugated AffiniPure Goat Anti-Rabbit/Mouse IgG H&L (cat. no. BA1056; 1:5,000) and HRP-Conjugated AffiniPure Donkey Anti-Rabbit IgG H&L (cat. no. BA1061; 1:2,000) (both Wuhan Boster Biological Technology, Co., Ltd.).

RNase R treatment. A total of 2 μg RNA was analyzed by incubation at 37˚C for 30 min with or without 5 U/μg RNase R (Epicenter; Illumina, Inc), following purification with an RNeasy MinElute Cleaning Kit (Qiagen GmbH), and then assessed using RT-qPCR.

Actinomycin D assay. The nerve cells in logarithmic growth stage were used, and when the cell density reached 80-90%, the adherent cells were enzymatically dissociated into a single-cell suspension. The neuronal cells were exposed to 2 μg/ml actinomycin D (MilliporeSigma). The cells were then collected and total RNA was withdrawn. circRNA and mRNA stability was analyzed using RT-qPCR.

Cell counting kit-8 (CCK-8) assay. The cells in each group following treatment were seeded in 96 well plates with a cell density of $2x10^4$ cells/well. Following 0, 24, and 48 h of culture, 10 μl CCK-8 solution (Beyotime Institute of Biotechnology) was added to each well. Following culture at 37˚C for 1.5 h, the absorbance of the cells at a wavelength of 450 nm was measured using an Elx800 reader (Omega Bio-Tek, Inc.) as a measure of the viability of the cells (28).

Flow cytometry assay. The OGD/R-treated neuronal cells were cultured for 48 h following transfection to assess apoptosis (18). After the culturing, cells were stained using an Annexin V FITC Apoptosis Detection Kit according to the manufacturer's protocol (BD Biosciences). The proportion of apoptotic cells in each group was analyzed using a flow cytometer (CytoFLEX; Beckman Coulter, Inc.). The flow data were analyzed by FlowJoTM v10.6.1 (BD Biosciences).

Dual-luciferase assay. The online tool StarBase (https://starbase.sysu.edu.cn/) was used to predict the putative miR-871 binding sites in circ_0000018 and BCL2L11. A fragment of circ_0000018 untranslated region (3'-UTR) with wild-type (circ_0000018-WT) and mutant (circ_0000018-MUT) was introduced into the pmirGLO luciferase vector (E1330, Promega Corporation). Similarly, the BLC2L11-3'-UTR fragment with wild type (BLC2L11-WT) and mutant (BLC2L11-MUT) was introduced into the pmirGLO luciferase vector. Lipofectamine® 3000 was used to co-transfect circ_0000018-WT/circ_0000018-MUT with BLC2L11-WT/BLC2L11-MUT and agomiR-871 or agomiR-NC into neuronal cells. Following transfection for 48 h, cells were collected, and the activity of luciferase was determined using a SpectraMax L fluorometer (Molecular Devices, LLC).

RNA pull-down assay. RNA pull-down assays were performed as previously reported (29). Briefly, neuronal cells ($1x10^7$ cells) were collected and lysed. Glycosylated miR-871 probes were synthesized by Shanghai GenePharma Co., Ltd. and cultured with streptavidin agarose beads (Thermo Fisher Scientific, Inc.). The cell lysate of the miR-871 probe or oligo probe (control) was incubated overnight at 4˚C. The bead-bound RNA complexes were purged with wash buffer, and the degree of enrichment of circ_0000018 extracted by the miR-871 probe was examined using RT-qPCR.

Statistical analysis. Data were analyzed using GraphPad Prism version 7.0 (GraphPad Software, Inc.). Comparisons

between two groups were performed using a Student's t-test, and comparisons between multiple groups were performed using a one-way ANOVA with a post-hoc Tukey's test. Data are presented as the mean ± standard deviation of three repeats.

Results

circ_0000018 levels in the in vivo AIS model. First, the GSE115697 dataset was downloaded from GEO and analyzed in R. The differentially expressed circRNAs in the tMCAO mice were obtained and expressed as a Volcano plot (Fig. 1A). Among these differentially expressed circRNAs, 10 circRNAs with the most notable differences in expression were selected and their levels in the OGD/R-treated cells were determined using RT-qPCR. The findings demonstrated that circ_0000018 and circ_0001646 levels were significantly increased in OGD/R treated cells compared with those in normal neuronal cells, while circ_0000018 levels were decreased. Of these two circRNAs, the difference in circ_0000018 levels expression was greater (Fig. 1B). Therefore, circ_0000018 was selected for subsequent experiments. In addition, following ribonuclease R (Fig. 1C) or actinomycin D (Fig. 1D) treatment, the linear RNA levels were significantly reduced, while no significant change was observed in circular RNA levels.

circ_0000018 downregulation relieves OGD/R-treated neuronal cell damage in vitro. To explore the effect of circ_0000018 *in vitro*, neuronal cells were transfected with si-circ_0000018 1#, si-circ_0000018 2#, or si-NC. The RT-qPCR results confirmed that transfection with siRNA plasmids targeting circ_0000018 markedly reduced the levels of circ_0000018 in neuronal cells, and si-circ_0000018 2# was selected for the subsequent experiments given the better knockdown efficiency (Fig. 2A). Furthermore, to explore the effects of circ_0000018 knockdown on AIS *in vitro*, an ODG/R cell model was established using transfected neuronal cells. CCK-8 assays showed that the knockdown of circ_0000018 markedly reduced neuronal cell activity (Fig. 2B). In addition, flow cytometry analysis indicated that apoptosis of neuronal cells was induced by OGD/R treatment, whereas circ_0000018 knockdown attenuated the apoptosis of OGD/R-stimulated neuronal cells (Fig. 2C).

Targeting association between circ_0000018 and miR-871. Using bioinformatics analysis, the top-7 miRNAs targeted by circ_0000018 were obtained. Next, based on PCR, only miR-871 expression was decreased in the OGD/R-treated neuronal cells (Fig. 3A). miR-871 was selected for further study. In Fig. 3B, the binding site between circ_0000018 and miR-871 is shown. Dual luciferase assays indicated that agomiR-871 markedly decreased the luciferase activity of the circ_0000018-wt reporter vector, with no influence on the MUT reporter vector (Fig. 3C). The RNA pull-down assays also showed that miR-871 and circ_0000018 could bind to each other (Fig. 3D). Furthermore, it was discovered that the levels of miR-871 were markedly increased in the OGD/R-treated neuronal cells transfected with si-circ_0000018 compared with cells transfected with si-NC (Fig. 3E). These findings

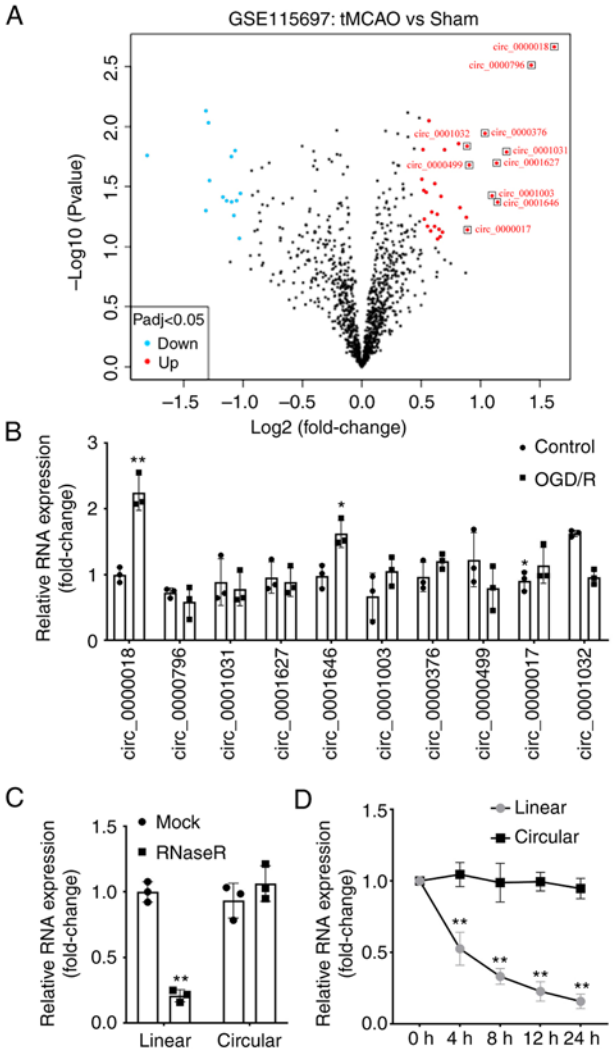

Figure 1. circ_0000018 levels in the *in vivo* model of AIS. (A) Differentially expressed circRNAs in the tMCAO GEO dataset (GSE115697). (B) Expression of 10 circRNAs in neuronal cells treated with or without OGD/R, as detected by RT-qPCR. *P<0.05, **P<0.01 vs. control. (C) Expression of linear RNAs and circRNAs following treatment with ribonuclease R, as detected by RT-qPCR. **P<0.01 vs. mock. (D) Expression of linear RNAs and circRNAs following treatment with actinomycin D were measured by RT-qPCR. **P<0.01 vs. circular. AIS, acute ischemic stroke; tMCAO, transient middle cerebral artery occlusion; OGD/R, oxygen-glucose deprivation; circRNA, circular RNA; RT-qPCR, reverse transcription-quantitative PCR.

revealed that circ_0000018 negatively regulated the expression of miR-871 by specifically binding to miR-871.

miR-871 downregulation alleviates the impact of circ_0000018 on the growth and apoptosis of OGD/R-treated neuronal cells. For the purpose of further investigating the roles of a circ_0000018/miR-871 axis on the injury of the OGD/R-treated cells, the OGD/R-treated neuronal cells were transfected with si-circ_0000018 and antogomiR-871. The transfection efficiency of antogomiR-871 was verified by RT-qPCR, and it was confirmed that antogomiR-871 transfection significantly decreased the miR-871 levels (Fig. 4A). The results of the CCK-8 assay indicated that si-circ_0000018 markedly reduced the survival of OGD/R-treated neuronal cells, while co-transfection with antagomiR-871 reduced this inhibitory effect (Fig. 4B). Similarly, the inhibitory effect on cell apoptosis induced by

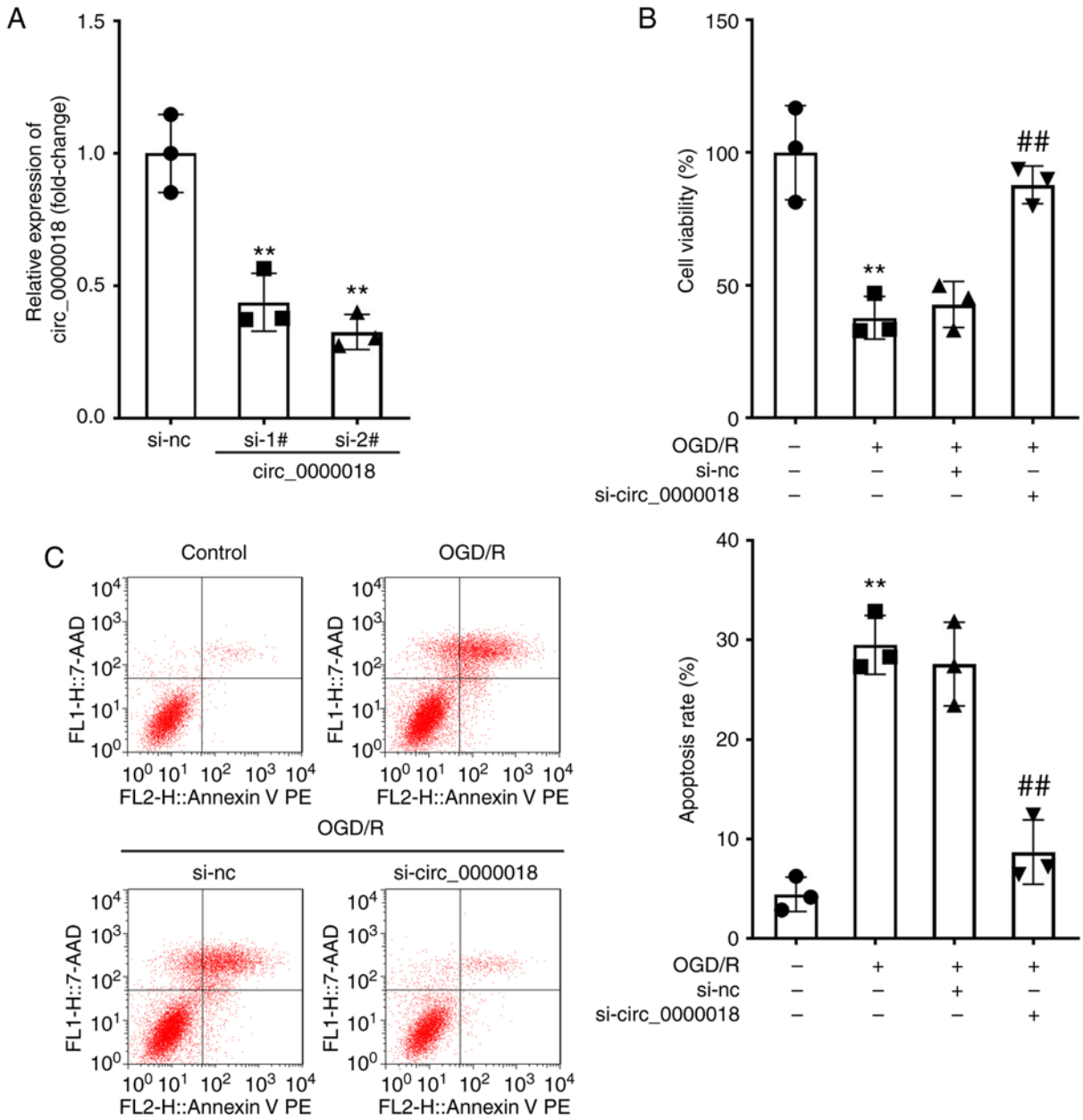

Figure 2. Downregulation of circ_0000018 reduces OGD/R-treated neuronal cell damage *in vitro*. (A) The levels of circ_0000018 were detected by RT-qPCR in neuronal cells transfected with si-circ_0000018 1#, si-circ_0000018 2#, and si-NC. (B) The function of circ_0000018 on the proliferation of neuronal cells, as detected using CCK-8 assays. (C) Cell apoptosis in OGD/R-treated neuronal cells transfected with si-circ_0000018 or si-NC, as evaluated using flow cytometry. **P<0.01 vs. control; $^{\#\#}$P<0.01 vs. OGD/R + si-NC. OGD/R, oxygen-glucose deprivation; circRNA, circular RNA; RT-qPCR, reverse transcription-quantitative PCR; CCK-8, cell counting kit-8.

circ_0000018 downregulation was markedly alleviated by antagomiR-871 in OGD/R-treated neuronal cells (Fig. 4C). Together, these results showed that downregulation of miR-871 can partially reverse the effects of si-circ_0000018 on the apoptosis and proliferation of neuronal cells following treatment with OGD/R. Proof of transfection for agomiR-871 and agomiR-NC in neuronal cells was obtained by RT-qPCR (Fig. S1A).

BCL2L11 is a target of miR-871. There is a general consensus that miRNAs exert their biological effects by targeting mRNAs (30-32). Therefore, StarBase was used to find potential target genes for miR-871. Several binding sites were obtained between miR-871 and BCL2L11 (Fig. 5A). Next, a dual luciferase assay performed in neuronal cells confirmed this binding relationship. The findings demonstrated that the upregulation of miR-871 markedly decreased the luciferase activity of the BCL2L11-wt reporter vector, whereas the luciferase activity of BCL2L11-mut was not decreased (Fig. 5B). The RNA pull-down assay demonstrated that miR-871 and BCL2L11 could specifically bind to each other (Fig. 5C). In addition, RT-qPCR and western blotting showed that the introduction of agtagomiR-871 decreased the effects of si-circ_0000018 on the mRNA levels of BCL2L11 in neuronal cells (Fig. 5D and F), revealing that circ_0000018 could regulate the levels of BCL2L11 by sponging miR-871. Consistently, it was found that BCL2L11 expression was increased in OGD/R-treated neuronal cells compared with the corresponding control group (Fig. 5E and G), which

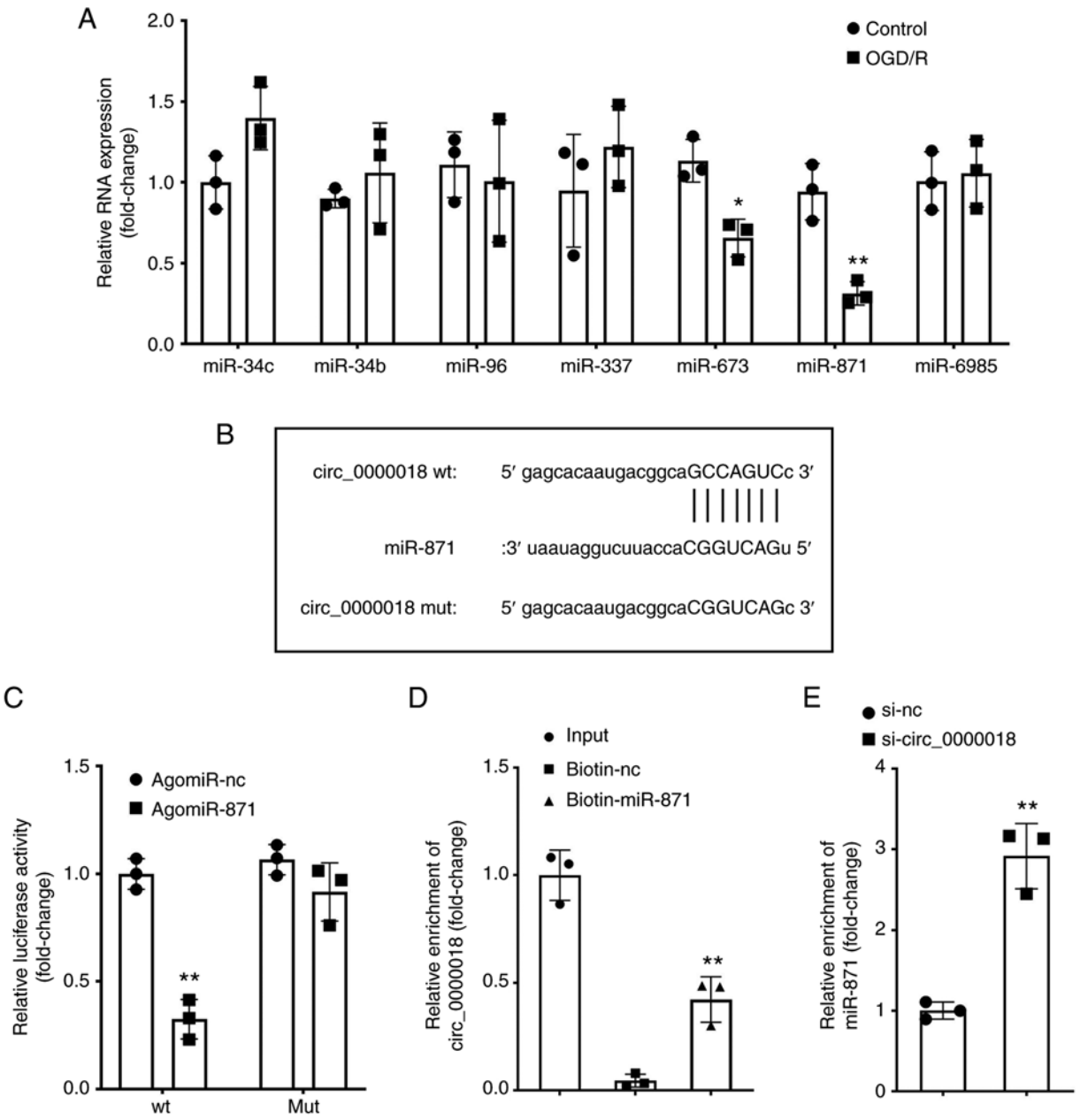

Figure 3. Targeting association between circ_0000018 and miR-871. (A) The levels of seven miRNAs in neuronal cells treated with or without OGD/R were tested by RT-qPCR. *P<0.05, **P<0.01 vs. control. (B) Binding sites for miR-871 exist in circ_0000018. (C) Luciferase activity was measured in neuronal cells co-transfected with circ_0000018-wt or circ_0000018-mut and agomiR-871 or agomiR-NC. **P<0.01 vs. agomiR-NC. (D) The targeting relationship between miR-871 and circ_0000018 was demonstrated by RNA pull-down assays. **P<0.01 vs. biotin-NC. (E) The levels of miR-871 were assessed in neuronal cells transfected with si-circ_0000018 or si-NC. **P<0.01 vs. si-NC. miRNA/miR, microRNA; OGD/R, oxygen-glucose deprivation; RT-qPCR, reverse transcription-quantitative PCR; circRNA, circular RNA.

demonstrated that BCL2L11 may be involved in OGD/R-treated cell trauma *in vitro*.

Overexpression of BCL2L11 reverses the effects of miR-871 on the growth and apoptosis of OGD/R-treated neuronal cells. To verify the potential influence of the circ_0000018/miR-871/BCL2L11 axis on the neuronal injury induced by ODG/R, rescue experiments were performed. Transfection efficiencies were determined by RT-qPCR (Fig. 6A and B). In addition, CCK-8 assays revealed that the proliferation of OGD/R-treated neuronal cells transfected with agomiR-871 was significantly increased, and this was abrogated by BCL2L11 overexpression (Fig. 6C). The flow cytometry results suggested that the treatment with ODG/R promoted apoptosis, whereas transfection of agomiR-871 in ODG/R-treated cells decreased apoptosis; further overexpression of BCL2L11 significantly reversed the effects of agomiR-871 on stimulating cell apoptosis (Fig. 6D).

circ_0000018 knockdown reduces cerebral ischemia/reperfusion injury in tMCAO mice. Finally, the contribution of circ_0000018 *in vivo* in the tMCAO mouse models was evaluated. RT-qPCR showed that circ_0000018 (Fig. 7A) and BCL2L11 (Fig. 7C) expression were significantly increased

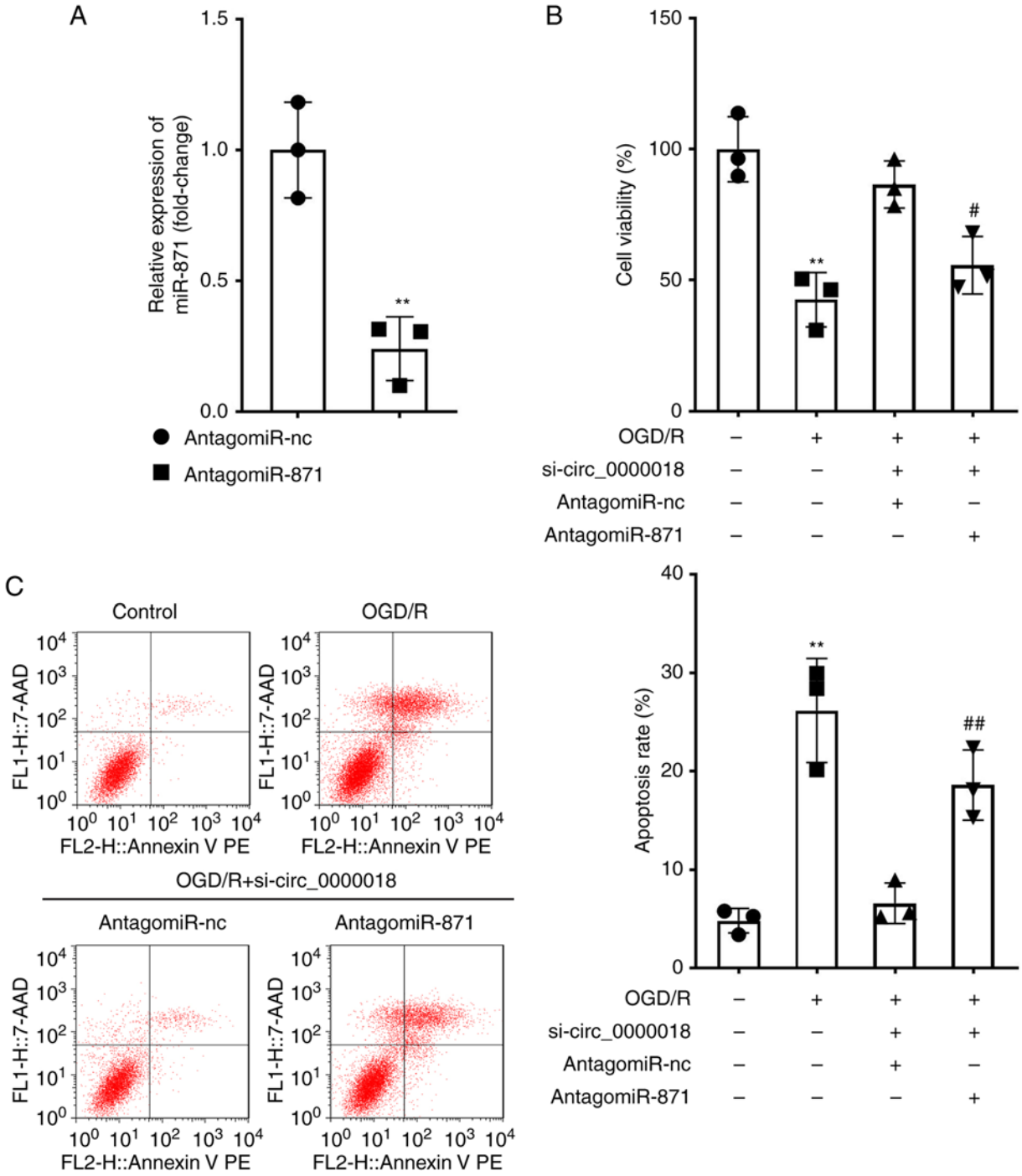

Figure 4. Downregulation of miR-871 alleviates the impact of circ_0000018 on the growth and apoptosis of OGD/R-treated neuronal cells. (A) Expression of miR-871 following transfection of OGD/R-treated neuronal cells with antagomiR-NC and antagomiR-871 were examined using RT-qPCR. **P<0.01 vs. antagomiR-NC. (B) The growth levels of neuronal cells treated with OGD/R were detected using CCK-8 assays. (C) Apoptosis of OGD/R-treated neuronal cells was investigated by flow cytometry. **P<0.01 vs. control; $^{\#}$P<0.05, $^{\#\#}$P<0.01 vs. OGD/R + si-circ_0000018 + antagomiR-NC. miR, microRNA; OGD/R, oxygen-glucose deprivation; RT-qPCR, reverse transcription-quantitative PCR; CCK-8, cell counting kit-8.

while miR-871 expression (Fig. 7B) was decreased in mouse brain tissues in the tMCAO group. Mice in the tMCAO group presented with increased neurological damage and brain infarction when compared with the sham group (Fig. 7D-F), and knockdown of circ_0000018 significantly ameliorated these changes. RT-qPCR results showed that the expression of circ_0000018 in tissues decreased after transfection with the plasmid with knockdown of circ_0000018 (Fig. S1B).

Discussion

Herein, OGD/R-treated neuronal cells and tMCAO mice were employed to investigate the function of circ_0000018. This study demonstrated that circ_0000018 levels were markedly increased both *in vitro* and *in vivo* in the AIS model and that the knockdown of circ_0000018 reduced the apoptosis of neuronal cells induced by OGD/R treatment. This indicated that circ_0000018 was involved in

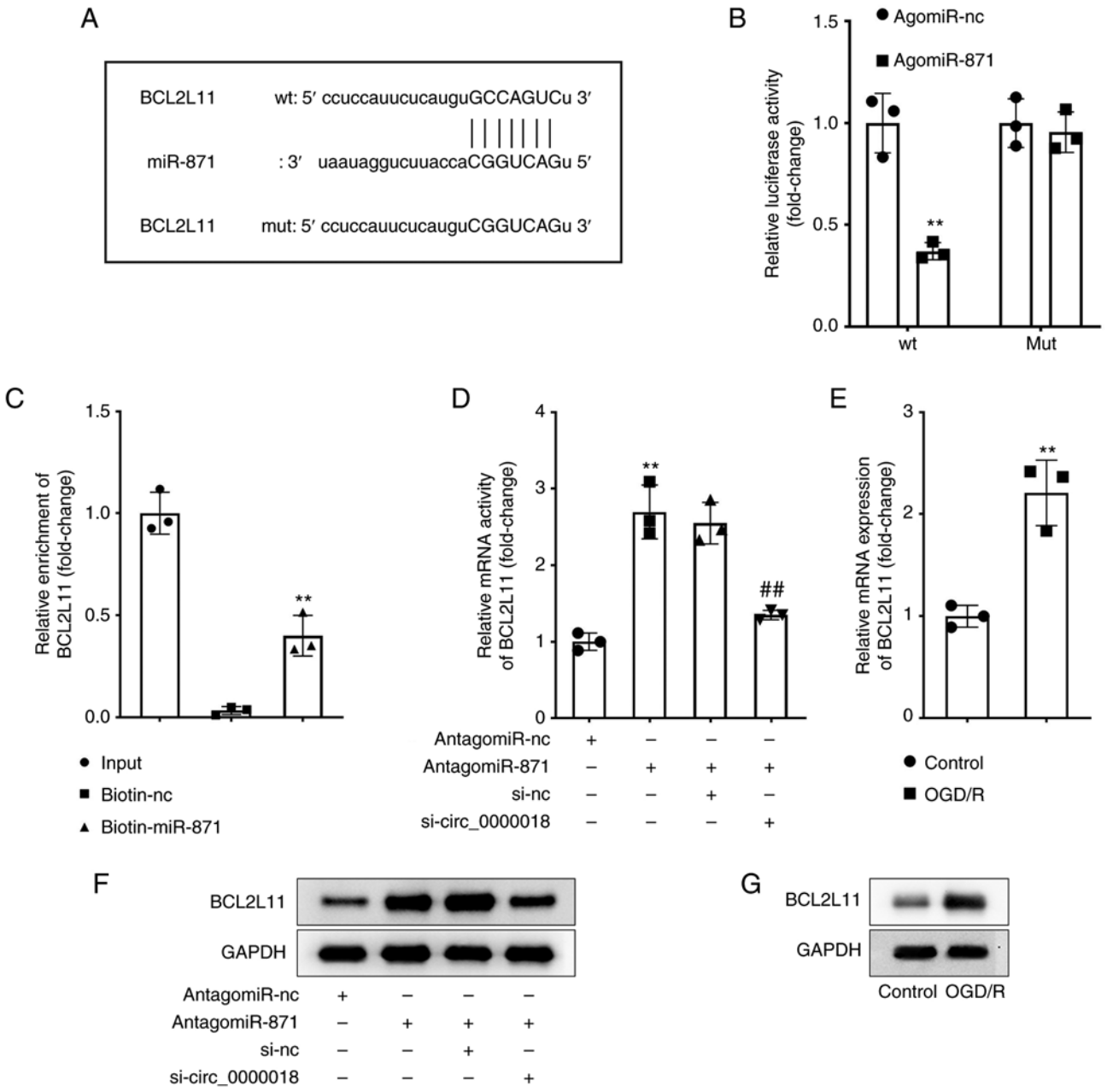

Figure 5. BCL2L11 acts as a target of miR-871. (A) The structure of the predicted binding site to miR-871 in the 3'-UTR sequence of BCL2L11 is shown in the schematic diagram. (B) The binding between miR-871 and BCL2L11 was confirmed using a dual luciferase reporter assay. **P<0.01 vs. agomiR-NC. (C) RNA pull-down assays were performed to validate the relationship between miR-871 and BCL2L11. **P<0.01 vs. biotin-NC. (D) The levels of BCL2L11 were assessed in neuronal cells transfected with antagomiR-NC, antagomiR-871, si-NC, and si-circ_0000018 using RT-qPCR. **P<0.01 vs. antagomiR-NC; $^{\#\#}$P<0.01 vs. antagomiR-871 + si-NC. (E) The levels of BCL2L11 were assessed in neuronal cells treated with or without OGD/R using RT-qPCR. **P<0.01 vs. control. (F) Western blotting was performed to determine the protein expression levels of BCL2L11 in neuronal cells transfected with antagomiR-NC, antagomiR-871, si-NC, and si-circ_0000018. (G) Western blotting was performed to determine the protein expression levels of BCL2L11 in neuronal cells treated with or without OGD/R. BCL2L11,Bcl-2-like protein 11; miR, microRNA; RT-qPCR, reverse transcription-quantitative PCR; OGD/R, oxygen-glucose deprivation; UTR, untranslated region.

the pathogenesis of AIS and may have potential as a novel therapeutic target.

According to recent studies, circRNAs not only exert significant effects in the regulation of gene expression but also take part in the pathogenesis of AIS. For instance, Mehta *et al* (33) studied the expressions profile of circ RNAs in the pneumonic cortex of MCAO mice at 6, 12, and 24 h after reperfusion by circRNA chip, and found that 283 circRNAs were significantly differentially expressed (based on a 2-fold change in expression). Bioinformatics analysis determined that 16/283 circRNAs were associated with a multitude of miRNA binding sites, as well as with stroke pathophysiology in a functional manner (33). In addition, Liu *et al* (34) also investigated the characteristics of circRNA expression in IS mouse tissue, and demonstrated that circRNA, such as mmu_circRNA_40001, mmu_circRNA_013120 and mmu_circRNA_40806 has the potential of becoming a target for the diagnosis and treatment of IS. Duan *et al* (35) more recently reported the characteristics of circRNA expression in rats following brain ischemia and examined the relationship between circRNA caused by

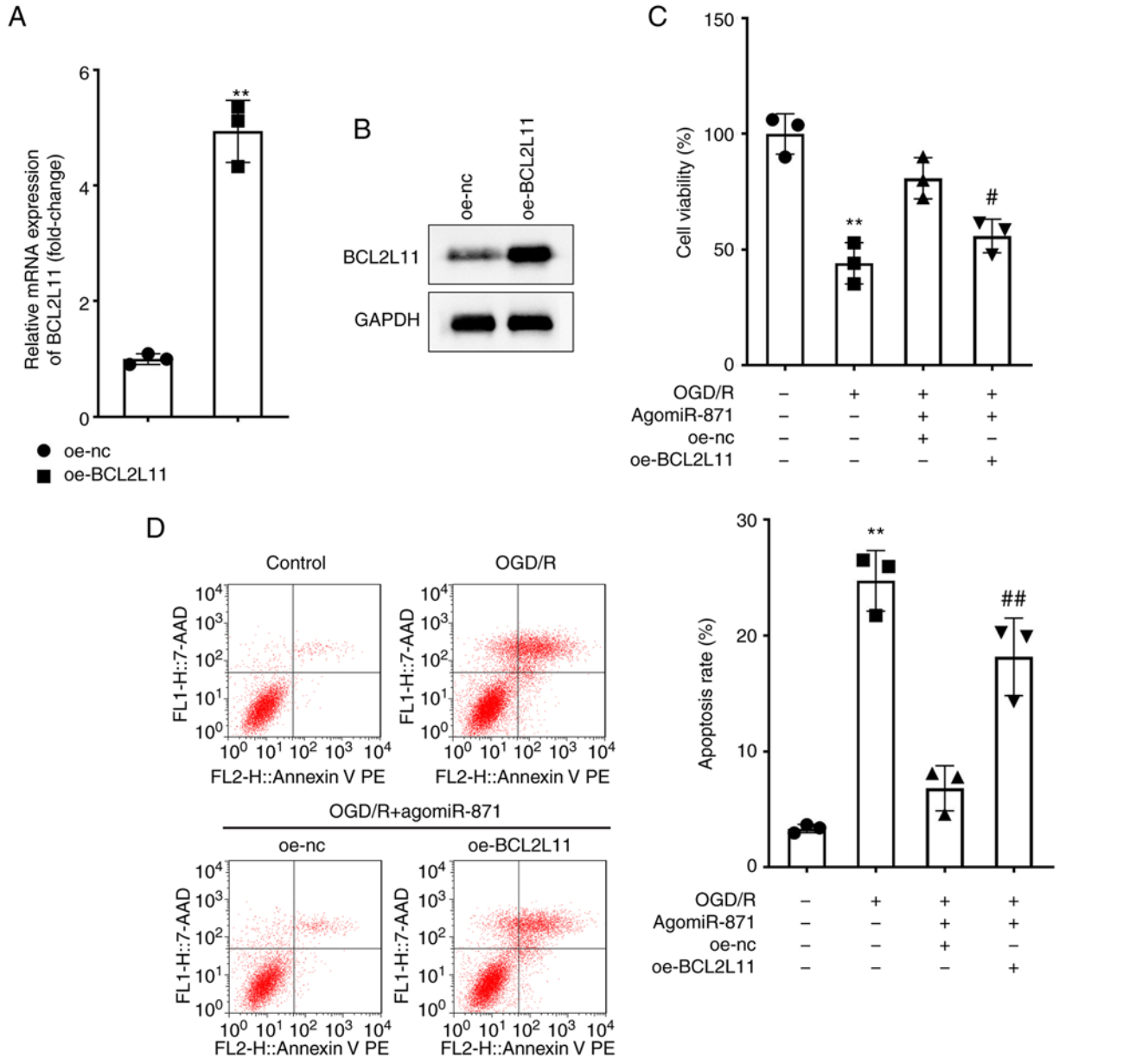

Figure 6. Overexpression of BCL2L11 reverses the effects of miR-871 on the growth and death of OGD/R-treated neuronal cells. (A) Expression of BCL2L11 following transfection with oe-NC and oe-BCL2L11 in neuronal cells was assessed by RT-qPCR. **P<0.01 vs. oe-NC. (B) Expression of BCL2L11 following transfection with oe-NC and oe-BCL2L11 in neuronal cells was detected by western blotting. (C and D) Neuronal cells were treated with control, OGD/R, OGD/R+agomiR-871+oe-NC, or OGD/R+agomiR-871+oe-BCL2L11. (C) Proliferation of neuronal cells was evaluated using a CCK-8 assay. (D) Apoptosis of neuronal cells following treatment was examined using flow cytometry. **P<0.01 vs. control; $^{\#}$P<0.05, $^{\#\#}$P<0.01 vs. OGD/R + agomiR-871 +oe-NC. BCL2L11, Bcl-2-like protein 11; miR, microRNA; OGD/R, oxygen-glucose deprivation; RT-qPCR, reverse transcription-quantitative PCR; CCK-8, cell counting kit-8; oe, overexpression; NC, negative control.

MCAO and IS in rats. Peng *et al* (10) reported the findings of a clinical investigation, which found that in peripheral blood mononuclear cells separated from blood samples in patients with AIS and healthy controls to detect the levels of circ_HECT domain E3 ubiquitin-protein ligase (HECTD), the levels of circ_HECTD were associated with a higher risk of disease, disease severity, inflammation, and recurrence of AIS. It is worth noting that the OGD/R-treated neuronal injury model has been extensively used to study circRNA in IS. circ_HECTD1 expression was decreased in OGD/R-treated mouse brain neuronal cells (HT-22), and the overexpression of circ_HECTD1 alleviated the death of OGD/R-treated HT-22 cells. Similarly, the present study demonstrated that circ_0000018 downregulation relieved OGD/R-treated neuronal cell damage *in vitro*.

There is substantial evidence to show that circRNAs exert various biological roles through their interactions with miRNAs (36,37). For example, circ_HECTD1 affected cellular injury following cerebral infarction by acting on the miR-27a-3p/FSTL1 axis (38). In addition, circ_0101874 overexpression increased the levels of phosphodiesterase 4D (PDE4D) by targeting miR-335-5p, which promoted neuronal damage in IS (39). To further validate the functional mechanism of circ_0000018 in the pathological process of AIS, the target mRNA, miR-871, was determined and validated. Luciferase reporter assays also showed the targeting

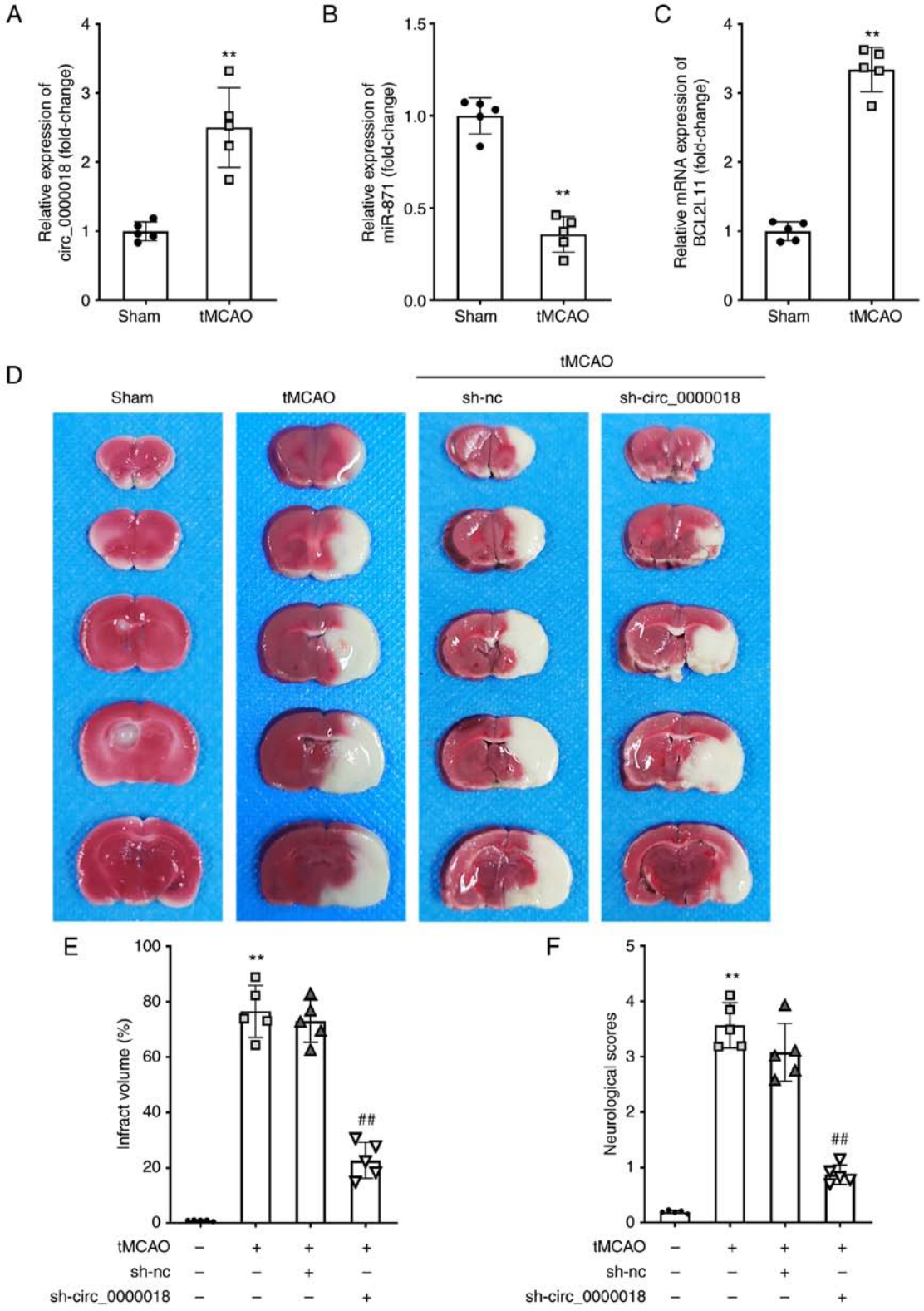

Figure 7. circ_0000018 knockdown relieves cerebral ischemia-reperfusion injury in tMCAO mice. (A-C) The levels of circ_0000018, miR-871, and BCL2L11 in cerebral tissue from tMCAO mice were examined using RT-qPCR. The mice were randomly allocated to a sham, tMCAO, tMCAO+sh-NC, or tMCAO+sh-circ_0000018 group (n=18, per group). **P<0.01 vs. sham. (D) TTC staining revealed focal ischemia induced by tMCAO in a typical brain section. (E) Following ischemia/reperfusion injury, the brain infarct volume in mice was analyzed using TTC staining. (F) Neurological impairment assessment. **P<0.01 vs. control; $^{\#\#}$P<0.01 vs. tMCAO + sh-NC. circRNA, circular RNA; tMCAO, transient middle cerebral artery occlusion; BCL2L11, Bcl-2-like protein 11; RT-qPCR, reverse transcription-quantitative PCR.

association between circ_0000018 and miR-871. Moreover, the downregulation of miR-871 reduced the suppressive functions of circ_0000018 knockdown on OGD/R-treated cell injury, which confirmed that the protective effect of circ_0000018 deficiency on AIS may be attributed, in part, to the association with miR-871. As a result, the inhibition of

miR-871 can reverse the effect of knockdown circ_0000018 on neuronal cells, suggesting that miR-871 may inhibit the development of AIS.

As a member of the BCL-2 protein family, BCL2L11 is located in the outer mitochondrial membrane, and plays an important regulatory role in mediating excitatory apoptosis, induction of gene sequence translocation, and mitochondrial depolarization (40,41). It was found that miR-29b inhibited the pro-apoptotic protein BCL2L11, Bcl-2 modifier, Bcl-2 interacting protein Harakir, and Bcl-2 binding component 3 (p53-upregulated modulator of apoptosis) during neuronal development, and played an essential role in neuronal maturation and inhibition of neuronal apoptosis (42). In the apoptotic pathway, Bax and Bcl-2 are two important regulatory genes; Bcl-2 inhibits cell death while Bax promotes it, and the ratio of Bcl-2/Bax is closely associated with the sensitivity of a cell to undergoing apoptosis (43). BCL2L11 has been validated as a key regulator of the apoptosis of B-lymphocytes, T-lymphocytes, macrophages, and granulocytes (44). Cheng *et al* (45) revealed the role of lncRNA-TUG1 in promoting neuronal apoptosis through the regulation of the miR-9/BCL2L11 axis in the context of cerebral ischemia, thus potentially providing a novel therapeutic target for stroke. Of note, in the present study, bioinformatics software predictions revealed that miR-871 has a conserved binding site in the 3'-UTR region of BCL2L11. The binding was further verified by luciferase reporter gene assays. Furthermore, the present study confirmed that BCL2L11 overexpression partially eliminated the inhibitory effect of miR-871 on OGD/R-treated neuronal cell injury. Furthermore, in neuronal cells, circ_00000018/miR-871 could regulate the expression of BCL2L11, which supports the regulatory functions of the circ_00000018/miR-871/BCL2L11 axis in AIS.

In conclusion, the findings of the present study indicated that circ_0000018, the expression of which was upregulated in the AIS model, may serve as a ceRNA for miR-871 to influence the levels of BCL2L11 and participate in the progression of AIS. Mechanistically, circ_0000018 knockdown relieved AIS *in vivo* and *in vitro* by regulating the miR-871/BCL2L11 axis. Thus, circ_0000018 may serve as a novel target for AIS treatment.

Acknowledgements

Not applicable.

Funding

No funding was received.

Availability of data and materials

The datasets used and/or analyzed during the current study are available from the corresponding author on reasonable request.

Authors' contributions

MJ and XBW conceived the study. MJ, XBW and SJ performed the experiments. MJ analyzed the data. MJ wrote the manuscript. All authors have read and approved the final manuscript. SJ and XBW confirm the authenticity of all the raw data.

Ethics approval and consent to participate

This study was approved by the Southeast University Animal Care and Use Committee (approval no. 20220110026).

Patient consent for publication

Not applicable.

Competing interests

The authors declare that they have no competing interests.

References

1. Feigin VL, Lawes CM, Bennett DA, Barker-Collo SL and Parag V: Worldwide stroke incidence and early case fatality reported in 56 population-based studies: A systematic review. Lancet Neurol 8: 355-369, 2009.
2. Inohara T, Liang L, Kosinski AS, Smith EE, Schwamm LH, Hernandez AF, Bhatt DL, Fonarow GC, Peterson ED and Xian Y: Recent myocardial infarction is associated with increased risk in older adults with acute ischemic stroke receiving thrombolytic therapy. J Am Heart Assoc 8: e012450, 2019.
3. Wang YJ, Li ZX, Gu HQ, Zhai Y, Jiang Y, Zhao XQ, Wang YL, Yang X, Wang CJ, Meng X, *et al*: China stroke statistics 2019: A report from the national center for healthcare quality management in neurological diseases, China national clinical research center for neurological diseases, the Chinese stroke association, national center for chronic and non-communicable disease control and prevention, Chinese center for disease control and prevention and institute for global neuroscience and stroke collaborations. Stroke Vasc Neurol 5: 211-239, 2020.
4. GBD 2019 Stroke Collaborators: Global, regional, and national burden of stroke and its risk factors, 1990-2019: A systematic analysis for the global burden of disease study 2019. Lancet Neurol 20: 795-820, 2021.
5. Chen Z, Jiang B, Ru X, Sun H, Sun D, Liu X, Li Y, Li D, Guo X and Wang W: Mortality of stroke and its subtypes in China: Results from a nationwide population-based survey. Neuroepidemiology 48: 95-102, 2017.
6. Jeck WR and Sharpless NE: Detecting and characterizing circular RNAs. Nat Biotechnol 32: 453-461, 2014.
7. Ebbesen KK, Kjems J and Hansen TB: Circular RNAs: Identification, biogenesis and function. Biochim Biophys Acta 1859: 163-168, 2016.
8. Ostolaza A, Blanco-Luquin I, Urdánoz-Casado A, Rubio I, Labarga A, Zandio B, Roldán M, Martínez-Cascales J, Mayor S, Herrera M, *et al*: Circular RNA expression profile in blood according to ischemic stroke etiology. Cell Biosci 10: 34, 2020.
9. Wu F, Han B, Wu S, Yang L, Leng S, Li M, Liao J, Wang G, Ye Q, Zhang Y, *et al*: Circular RNA TLK1 aggravates neuronal injury and neurological deficits after ischemic stroke via miR-335-3p/TIPARP. J Neurosci 39: 7369-7393, 2019.
10. Peng X, Jing P, Chen J and Xu L: The role of circular RNA HECTD1 expression in disease risk, disease severity, inflammation, and recurrence of acute ischemic stroke. J Clin Lab Anal 33: e22954, 2019.
11. Van Rooij E, Purcell AL and Levin AA: Developing micro RNA therapeutics. Circ Res 110: 496-507, 2012.
12. Ghoreishy A, Khosravi A and Ghaemmaghami A: Exosomal microRNA and stroke: A review. J Cell Biochem 120: 16352-16361, 2019.
13. Chen Y, Gao C, Sun Q, Pan H, Huang P, Ding J and Chen S: MicroRNA-4639 is a regulator of DJ-1 expression and a potential early diagnostic marker for Parkinson's disease. Front Aging Neurosci 9: 232, 2017.
14. Arena A, Iyer AM, Milenkovic I, Kovacs GG, Ferrer I, Perluigi M and Aronica E: Developmental expression and dysregulation of miR-146a and miR-155 in Down's syndrome and mouse models of Down's syndrome and Alzheimer's disease. Curr Alzheimer Res 14: 1305-1317, 2017.

15. Beveridge NJ, Tooney PA, Carroll AP, Gardiner E, Bowden N, Scott RJ, Tran N, Dedova I and Cairns MJ: Dysregulation of miRNA 181b in the temporal cortex in schizophrenia. Hum Mol Genet 17: 1156-1168, 2008.
16. Jeyaseelan K, Lim KY and Armugam A: MicroRNA expression in the blood and brain of rats subjected to transient focal ischemia by middle cerebral artery occlusion. Stroke 39: 959-966, 2008.
17. Dharap A, Bowen K, Place R, Li LC and Vemuganti R: Transient focal ischemia induces extensive temporal changes in rat cerebral microRNAome. J Cereb Blood Flow Metab 29: 675-687, 2009.
18. Liu DZ, Tian Y, Ander BP, Xu H, Stamova BS, Zhan X, Turner RJ, Jickling G and Sharp FR: Brain and blood microRNA expression profiling of ischemic stroke, intracerebral hemorrhage, and kainate seizures. J Cereb Blood Flow Metab 30: 92-101, 2010.
19. Abe A, Tanaka M, Yasuoka A, Saito Y, Okada S, Mishina M, Abe K, Kimura K and Asakura T: Changes in whole-blood microRNA profiles during the onset and treatment process of cerebral infarction: A human study. Int J Mol Sci 21: 3107, 2020.
20. Han B, Zhang Y, Zhang Y, Bai Y, Chen X, Huang R, Wu F, Leng S, Chao J, Zhang JH, *et al*: Novel insight into circular RNA HECTD1 in astrocyte activation via autophagy by targeting MIR142-TIPARP: Implications for cerebral ischemic stroke. Autophagy 14: 1164-1184, 2018.
21. R Core Team: R: A language and environment for statistical computing. R Foundation for Statistical Computing, Vienna, Austria. ISBN 3-900051-07-0, 2012.
22. RStudio Team: Rstudio: Integrated development for R. Rstudio, Inc., Boston, MA, 2015.
23. Liu W, Miao Y, Zhang L, Xu X and Luan Q: MiR-211 protects cerebral ischemia/reperfusion injury by inhibiting cell apoptosis. Bioengineered 11: 189-200, 2020.
24. Wibrand K, Pai Bl, Siripornmongcolchai T, Bittins M, Berentsen B, Ofte ML, Weigel A, Skaftnesmo KO and Bramham CR: MicroRNA regulation of the synaptic plasticity-related gene Arc. PLoS One 7: e41688, 2012.
25. Fiore R, Khudayberdiev S, Christensen M, Siegel G, Flavell SW, Kim TK, Greenberg ME and Schratt G: Mef2-mediated transcription of the miR379-410 cluster regulates activity-dependent dendritogenesis by fine-tuning Pumilio2 protein levels. EMBO J 28: 697-710, 2009.
26. Magill ST, Cambronne XA, Luikart BW, Lioy DT, Leighton BH, Westbrook GL, Mandel G and Goodman RH: microRNA-132 regulates dendritic growth and arborization of newborn neurons in the adult hippocampus. Proc Natl Acad Sci USA 107: 20382-20387, 2010.
27. Livak KJ and Schmittgen TD: Analysis of relative gene expression data using real-time quantitative PCR and the 2(-Delta Delta C(T)) method. Methods 25: 402-408, 2001.
28. Olde Loohuis NFM, Kos A, Martens GJM, Van Bokhoven H, Nadif Kasri N and Aschrafi A: MicroRNA networks direct neuronal development and plasticity. Cell Mol Life Sci 69: 89-102, 2012.
29. Broderick JA and Zamore PD: MicroRNA therapeutics. Gene Ther 18: 1104-1110, 2011.
30. Hu J, Xie C, Xu S, Pu Q, Liu H, Yang L, Wang W, Mao L, Li Z and Chen W: Liver fibrosis-derived exosomal miR-106a-5p facilitates the malignancy by targeting SAMD12 and CADM2 in hepatocellular carcinoma. PLoS One 18: e0286017, 2023.
31. Tuo X, Zhou Y, Yang X, Ma S, Liu D, Zhang X, Hou H, Wang R, Li X and Zhao L: miR-532-3p suppresses proliferation and invasion of ovarian cancer cells via GPNMB/HIF-1α/HK2 axis. Pathol Res Pract 237: 154032, 2022.
32. Cheng Q, Chen M, Wang H, Chen X, Wu H, Du Y and Xue J: MicroRNA-27a-3p inhibits lung and skin fibrosis of systemic sclerosis by negatively regulating SPP1. Genomics 114: 110391, 2022.
33. Mehta SL, Pandi G and Vemuganti R: Circular RNA expression profiles alter significantly in mouse brain after transient focal ischemia. Stroke 48: 2541-2548, 2017.
34. Liu C, Zhang C, Yang J, Geng X, Du H, Ji X and Zhao H: Screening circular RNA expression patterns following focal cerebral ischemia in mice. Oncotarget 8: 86535-86547, 2017.
35. Duan X, Li L, Gan J, Peng C, Wang X, Chen W and Peng D: Identification and functional analysis of circular RNAs induced in rats by middle cerebral artery occlusion. Gene 701: 139-145, 2019.
36. Hansen TB, Jensen TI, Clausen BH, Bramsen JB, Finsen B, Damgaard CK and Kjems J: Natural RNA circles function as efficient microRNA sponges. Nature 495: 384-388, 2013.
37. Dai Q, Ma Y, Xu Z, Zhang L, Yang H, Liu Q and Wang J: Downregulation of circular RNA HECTD1 induces neuroprotection against ischemic stroke through the microRNA-133b/TRAF3 pathway. Life Sci 264: 118626, 2021.
38. Pei L, Xu X and Yuan T: Circ_0101874 overexpression strengthens PDE4D expression by targeting miR-335-5p to promote neuronal injury in ischemic stroke. J Stroke Cerebrovasc Dis 31: 106817, 2022.
39. Zhang Z, He J and Wang B: Circular RNA circ_HECTD1 regulates cell injury after cerebral infarction by miR-27a-3p/FSTL1 axis. Cell Cycle 20: 914-926, 2021.
40. Concannon CG, Tuffy LP, Weisová P, Bonner HP, Dávila D, Bonner C, Devocelle MC, Strasser A, Ward MW and Prehn JH: AMP kinase-mediated activation of the BH3-only protein Bim couples energy depletion to stress-induced apoptosis. Cell Biol 189: 83-94, 2010.
41. Kilbride SM, Farrelly AM, Bonner C, Ward MW, Nyhan KC, Concannon CG, Wollheim CB, Byrne MM and Prehn JH: AMP-activated protein kinase mediates apoptosis in response to bioenergetic stress through activation of the pro-apoptotic Bcl-2 homology domain-3-only protein BMF. J Biol Chem 285: 36199-36206, 2010.
42. Ouyang YB, Xu L, Lu Y, Sun X, Yue S, Xiong XX and Giffard RG: Astrocyte-enriched miR-29a targets PUMA and reduces neuronal vulnerability to forebrain ischemia. Glia 61: 1784-1794, 2013.
43. Liu L, Liu Y, Zhang T, Wu H, Lin M, Wang C, Zhan Y, Zhou Q, Qiao B, Sun X, *et al*: Synthetic Bax-Anti Bcl2 combination module actuated by super artificial hTERT promoter selectively inhibits malignant phenotypes of bladder cancer. Exp Clin Cancer Res 35: 3, 2016.
44. Strasser A: The role of BH3-only proteins in the immune system. Nat Rev Immunol 5: 189-200, 2005.
45. Chen S, Wang M, Yang H, Mao L, He Q, Jin H, Ye ZM, Luo XY, Xia YP and Hu B: LncRNA TUG1 sponges microRNA-9 to promote neurons apoptosis by up-regulated Bcl2l11 under ischemia. Biochem Biophys Res Commun 485: 167-173, 2017.